Visualization of mRNA translation in living cells

Alexis J. Rodriguez, Shailesh M. Shenoy, Robert H. Singer, and John Condeelis

Department of Anatomy and Structural Biology, Albert Einstein College of Medicine, Bronx, NY 10461

The role of mRNA localization is presumably to effect cell asymmetry by synthesizing proteins in specific cellular compartments. However, protein synthesis has never been directly demonstrated at the sites of mRNA localization. To address this, we developed a live cell method for imaging translation of β-actin mRNA. Constructs coding for β-actin, containing tetracysteine motifs, were transfected into C2C12 cells, and sites of nascent polypeptide chains were detected using the biarsenial dyes FlAsH and ReAsH, a technique we call translation site imaging. These sites colocalized with β-actin mRNA at the leading edge of motile myoblasts, confirming that they were translating. β-Actin mRNA lacking the sequence (zipcode) that localizes the mRNA to the cell periphery, eliminated the translation there. A pulse-chase experiment on living cells showed that the recently synthesized protein correlated spatially with the sites of its translation. Additionally, localization of β-actin mRNA and translation activity was enhanced at cell contacts and facilitated the formation of intercellular junctions.

Introduction

mRNA localization is a critical step in the development of cellular asymmetry. This suggests that controlling sites of translation restricts target proteins to specific subcellular compartments (Bashirullah et al., 1998; Zhang et al., 2001). For instance, mRNA localization is required during development to establish morphogen gradients in the oocyte and for cell lineage specification in the early embryo (Rodriguez et al., 2005). mRNA localization to distal regions of neurons has been observed, and local translation of these mRNAs can be initiated in response to various extracellular cues (Tiruchinapalli et al., 2003). The ability to determine where translation occurs may provide clues to the spatial and temporal organization of cells and tissues by elucidating the relationship between localized mRNAs and the distribution of protein products of translation. Where translation occurs relative to extracellular cues is critical to understanding how cells chemotax in response to their environment, a process that is critical to understanding how cells within a tumor make the decision to metastasize (Wang et al., 2004). During neuronal development, determining the sites of translation of specific proteins may be critical in understanding how neurons find their proper targets for synapse formation through the regulation of growth cone assembly and movement. In addition, monitoring the sites of translation of specific mRNAs in the pre- and postsynaptic regions of neurons may elucidate how cells convert electrical stimulation into stored memory, the process of synaptic plasticity.

Correspondence to Alexis J. Rodriguez: arodrigu@aecom.yu.edu

Abbreviations used in this paper: EDT_2; ethanedithiol; FL, full-length; TC, tetracysteine; ZBP1, zipcode binding protein 1.

The online version of this article contains supplemental material.

One of the better characterized models of mRNA localization is the process used by β-actin. The localization of β-actin mRNA is correlated with the localization of β-actin protein to apical structures such as filaments in microvilli of epithelia and auditory hair cells and the leading edge of lamellipodia and filopodia of crawling cells (Hofer et al., 1997; Shestakova et al., 2001).

Zipcode sequences are components of localized mRNAs that are necessary and sufficient for the proper targeting of transcripts. The β-actin zipcode is responsible for the localization of β-actin mRNA to the periphery of fibroblasts or the growth cone of neuronal cells (Kislauskis et al., 1993; Zhang et al., 1999). The concept that β-actin contributes to leading edge dynamics is supported by the observation that β-actin mRNA targeting to the front of crawling cells is necessary for directed motility of fibroblasts and carcinoma cells (Kislauskis et al., 1994; Shestakova et al., 1999; Wang et al., 2004). Inhibition of β-actin mRNA targeting, by using antisense oligonucleotides directed to the zipcode or by deleting the zipcode, resulted in a decrease in cell speed and directionality (Kislauskis et al., 1997; Shestakova et al., 2001). Inhibition of β-actin mRNA targeting by using antisense oligonucleotides also resulted in the randomization of the location of free barbed ends in the cell cortex, suggesting that the sites of β-actin polymerization are determined in part by the localization of its mRNA (Shestakova et al., 2001).

Although these reports emphasize the fundamental role of RNA localization, it has not been established how cell physiology is mechanistically related to the compartmentalized synthesis of proteins. To do so will require a means to follow newly synthesized proteins from their sites of translation to their sites of utilization. Therefore, we developed a method

The Journal of Cell Biology, Vol. 175, No. 1, October 9, 2006 67–76
http://www.jcb.org/cgi/doi/10.1083/jcb.200512137

called translation site imaging for identifying polypeptides as they are synthesized in living cells and released to their sites of utilization. The approach can simultaneously detect β-actin mRNA, translation sites, and mature protein in living cells based on genetically encodable tetracysteine (TC) tags that associate with the biarsenical dyes FlAsH and ReAsH (Zhang et al., 2002).

Results

To identify sites of β-actin translation, β-actin promoter–driven constructs were generated to ensure the proper copy number of total actin transcripts. A TC tag (CCPGCC) was inserted at the N terminus, followed by a GFP fusion domain and the β-actin coding sequence, with or without the 3′UTR zipcode sequence. The construct that contains the β-actin 3′UTR and, thus, the zipcode will be referred to as the full-length (FL) construct, whereas the constructs that lacks the β-actin 3′UTR containing the zipcode will be referred to as the ΔZIP construct. After ReAsH staining, C2C12 cells transfected with the FL construct exhibited a staining pattern nearly identical to that of GFP–β-actin (Fig. 1, B and C). C2C12 myoblasts were used for these investigations based on their ability to target β-actin mRNA (Hill and Gunning, 1993). In addition, these cells differentiate into muscle through fusion of cell contacts, a process that we were interested in investigating with regard to a potential role for localized translation at contacts.

By using the concentration of nascent polypeptide chains at polysome sites, we expected to identify translation sites using ReAsH staining and the translation elongation inhibitor cycloheximide (Fig. 1 D). Cycloheximide is known to accumulate ribosomes and nascent polypeptide chains on mRNA (Godchaux et al., 1967; Lodish, 1971). ReAsH staining of C2C12 cells transfected with the FL construct resulted in the detection of discrete uniformly sized bright puncta generally localized at the cell periphery, even without cycloheximide (Fig. 2, C and D). Their distribution was similar to that of β-actin mRNA in mouse myoblast cells (Hill and Gunning, 1993). Untransfected cells did not exhibit punctate staining (not depicted), indicating that the observed ReAsH puncta resulted specifically from the binding of dye to the transgene protein product. When cells containing the ΔZIP construct

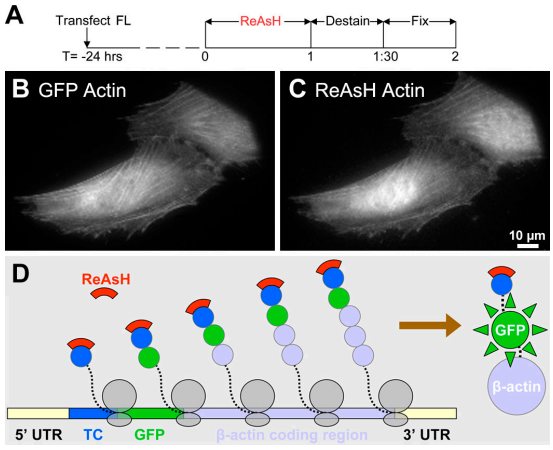

Figure 1. **ReAsH labeling of the TC motif in the absence of cycloheximide results in a pattern similar to GFP–β-actin.** (A) Schematic representation of the time course of the procedure used in B and C. (B) Epifluorescence image of the distribution of GFP–β-actin from a C2C12 cell transfected with the FL construct. (C) Epifluorescence image of ReAsH staining from the cell in B. Note the similarity between the staining patterns in the absence of cycloheximide (compare B and C). (D) Model of the translation site detection scheme. ReAsH (red) will label the TC motif of nascent chains of β-actin and mature β-actin, whereas GFP will only label mature β-actin protein. ReAsH staining of cells containing the TC–GFP–β-actin constructs performed in the presence of cycloheximide should increase the number of nascent chains at the polysome site as the rate of ribosomal translocation decreases, providing a more robust and persistent fluorescence signal, resulting in bright red puncta at the sites of translation. Ribosome packing is not to scale. Bar, 10 μm.

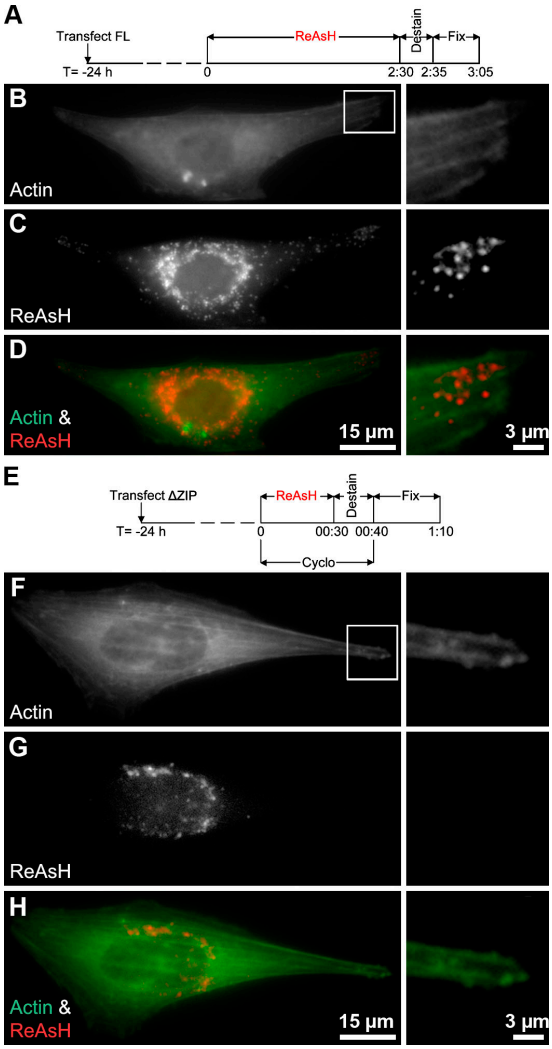

Figure 2. **ReAsH labeling reveals the sites of β-actin translation.** Epifluorescence images of C2C12 cells containing the FL (B–D) or ΔZIP (F–H) construct stained with ReAsH. (A) Schematic representation of the time course of the procedure used in B–D. (E) Schematic representation of the time course of the procedure used in F–H. (B and F) Epifluorescence image showing the distribution of mature GFP–β-actin with a close up of the boxed region shown in the inset. (C and G) Epifluorescence image showing numerous bright puncta in the red channel, representing the distribution of nascent chains of β-actin throughout the cell. (D and H) Overlay of the images, showing the proximity between the red nascent chains and green actin filaments.

were stained with ReAsH, puncta were observed in the perinuclear region and very few were observed at the cell periphery, suggesting that the information contained within the zipcode region is responsible not only for the proper targeting of mRNA but also for proper targeting of the translation sites (Fig. 2, G and H). These data also demonstrate that translation sites can be detected after ReAsH staining by quick destaining and fixation (Fig. 2, A–D) or by the use of cycloheximide during staining and destaining (Fig. 2, E–H).

Intact polysomes are required for the detection of translation sites

To demonstrate that the puncta are a result of translation, we treated the cells with puromycin, a reagent known to dissociate ribosomes and nascent chains from mRNAs (Yarmolinsky and De la Haba, 1959; Joklik and Becker, 1965). As described, cells expressing the FL construct treated with cycloheximide and subsequently stained with ReAsH exhibited more numerous puncta throughout the cytoplasm than nontreated cells, consistent with the increased loading of nascent chains known to occur after this treatment (Singer and Penman, 1972; Fig. 3 A). In contrast, cells pretreated with puromycin, before cycloheximide, exhibited a decrease in the number of puncta, consistent with the dissociation of nascent chains known to occur after this treatment (Fig. 3 B). Quantification of the relative number of puncta/cell for the puromycin-treated cells compared with the cells with only cycloheximide showed an approximately sevenfold reduction (Fig. 3 C). These data indicate that intact polysomes are needed for the detection of the puncta after ReAsH staining and represent translation sites based on their sensitivity to translational inhibitors.

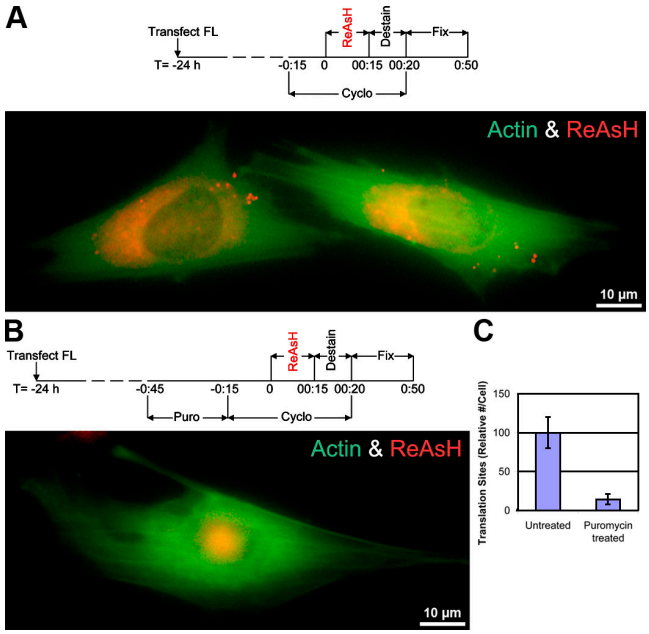

Figure 3. **Disrupting polysome structure with puromycin prevents the detection of ReAsH sites.** (A) Overlay image of cells stained with ReAsH in the presence of 100 µg/ml cycloheximide showing GFP–β-actin (green) and ReAsH staining (red) with a schematic representation of the time course of the procedure. Notice the presence of numerous ReAsH puncta throughout the cytoplasm. (B) Overlay image of a cell pretreated with 200 µg/ml puromycin stained with ReAsH in the presence of 100 µg/ml cycloheximide showing GFP–β-actin (green) and ReAsH staining (red) with a schematic representation of the time course of the procedure. Notice the absence of any ReAsH puncta caused by the pretreatment with puromycin. (C) Graph of the relative number of ReAsH puncta per cell in cells treated with and without puromycin where the data are normalized to the number of puncta in the untreated sample. The disruption of polysomes leads to an approximately sevenfold reduction in the number of ReAsH puncta per cell as compared with control cells ($P = 0.005$). Untreated population, $n = 5$; puromycin-treated population, $n = 8$. Error bars are ± SEM.

Translation sites are transient in living cells

We would expect the nascent chains to "run off" after removing ReAsH. To investigate this, live cells were imaged after the removal of the ReAsH dye solution to determine the persistence of the puncta (Fig. 4). The translation sites were observed for ~5 min after ReAsH removal before the signal reached background levels (Fig. 4 A). Pretreatment with cycloheximide prolonged the persistence of the signal to >45 min (Fig. 4 B). These data suggest that the ReAsH-stained nascent chains continued to elongate because, in cells lacking cycloheximide, sites disappeared after a few minutes, consistent with the release of the nascent chains labeled with ReAsH and their replacement by nonlabeled nascent chains. The sites persisted for at least 45 min in the presence of cycloheximide because the nascent chains with bound ReAsH remained associated with polysomes because of the elongation block.

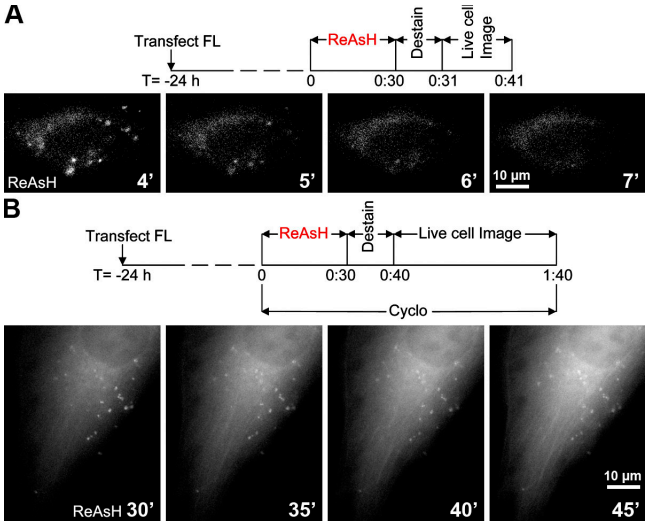

Figure 4. **Prolonged imaging of translation sites requires inhibition of translational elongation.** (A) A live ReAsH-stained C2C12 cell transfected with the FL construct has bright puncta for 5 min before the signal is no longer detectable because of "run off" of the labeled nascent polypeptides. The images were a time-lapse series taken every minute starting at 4 min. A schematic representation of the time course of the procedure is provided. (B) In the presence of cycloheximide, an image of a live ReAsH-stained C2C12 cell transfected with the FL construct has bright puncta (translation sites) at 30 min that are still present in the same location after 45 min after removal of ReAsH. A schematic representation of the time course of the procedure is provided. See Video 1 (available at http://www.jcb.org/cgi/content/full/jcb.200512137/DC1).

The localization of mRNA, translation sites, and mature protein are spatially correlated at the cellular periphery and require the zipcode

Actively translating mRNA should colocalize with sites of ReAsH staining. Fluorescence in situ hybridization experiments were performed on C2C12 cells transfected with the FL or ΔZIP construct. When cells expressing the FL construct were hybridized with probes against the GFP coding sequence, mRNA was observed throughout the cell, including the periphery (Fig. 5 A). In contrast, cells containing the ΔZIP construct did not efficiently target GFP–β-actin mRNA to the cell periphery (Fig. 5 B). To compare the localization of the RNA in the two populations, the fluorescence intensity as a function of distance from the nucleus was compared among cells expressing either the FL construct or the ΔZIP construct (Fig. 5 C). For the population of cells with the FL construct, fluorescence extended to the cell periphery (Fig. 5 C, red line). In contrast, the ΔZIP construct was prevalent in the perinuclear region with a significant decrease at the cell periphery (Fig. 5 C, blue line).

Translation sites were also observed at the periphery of cells with the FL construct (Fig. 5 D, red line). In contrast, when the sites of translation for a population of cells expressing the ΔZIP transgene were analyzed as a function of relative distance from the nucleus, fluorescence at the cell periphery was not detected (Fig. 5 D, blue line). Likewise, the distribution of the GFP signal, representing synthesized protein, also showed asymmetric localization, similar to that observed for mRNA localization (Fig. 5, compare C and E). Thus, the zipcode appeared to be required for targeted β-actin mRNA to be translated at the cell periphery and β-actin protein to accumulate there.

It has been suggested that mRNAs are translated when associated with the cytoskeleton (Lenk et al., 1977). To investigate whether the sites of translation were associated with the cytoskeleton, saponin-extracted C2C12 cells expressing the FL construct were stained with ReAsH. Fluorescence imaging confirmed that translation sites remained after detergent extraction, suggesting that they were associated with the detergent-resistant cytoskeleton (Fig. S1, available at http://www.jcb.org/cgi/content/full/jcb.200512137/DC1). To further investigate the anchoring of β-actin translation sites, time-lapse imaging of C2C12 cells stained with ReAsH was performed (Video 1). Analysis of the position of the identified translation sites indicated that there was very little movement of these sites during the time course of the experiment, consistent with the hypothesis that translating mRNAs are anchored to the cytoskeleton. In contrast, directed movements of reporter mRNAs are measured at rates on the order of 1 μm/s, indicating that the translation sites are not a subset of directed mRNAs (Fusco et al., 2003). Importantly, cells treated with the translational inhibitor cycloheximide for up to 3 h are able to target mRNA properly, suggesting that the lack of movement observed in the time-lapsed images was not due to an effect of the cycloheximide treatment on mRNA movements (Sundell and Singer, 1990).

Nascent chain colocalization with mRNA at cell–cell contacts requires the zipcode and results in the local accumulation of newly synthesized protein

Overlay images of ReAsH and FISH images showed that colocalization between the red translation sites and green mRNAs were often near cell–cell contacts when the C2C12 cells contained the FL construct (Fig. 6, left). The majority of mRNAs not at cell contacts were not translating, suggesting that the contact between cells created an environment that enhanced localized translation (Fig. 6 J). In contrast, when contacting cells containing the ΔZIP construct were imaged, translation sites

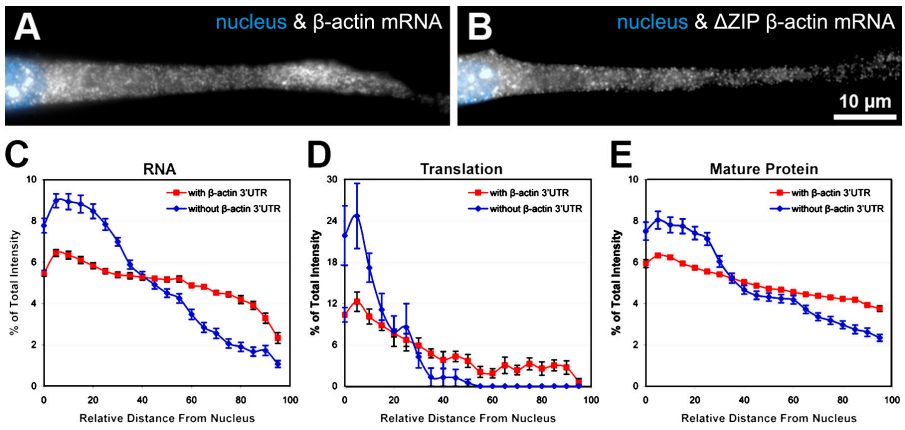

Figure 5. **Localization of the β-actin mRNA transgene correlates with the distribution of mature protein and translation sites.** Fluorescence in situ hybridization experiments were performed on C2C12 cells transfected with the FL or ΔZIP construct with Cy-5–labeled probes against the GFP coding sequence. (A) Overlay image of a C2C12 cell transfected with the FL construct showing localized β-actin transgene mRNA at the cell periphery as assessed by a probe for GFP (white) and DAPI staining of the nucleus (blue). (B) Overlay image of a C2C12 cell transfected with the ΔZIP construct showing the β-actin transgene mRNA levels highest near the nucleus and dropping off toward the cell periphery as assessed by a probe for GFP (white) and DAPI staining of the nucleus (blue). (C) The relative intensity as a function of distance from the nucleus of the Cy-5–labeled probe for GFP was determined for a population of C2C12 cells containing the FL or ΔZIP construct (see Materials and methods). The fluorescence intensity as a function of normalized distance (the percentage of distance from the nucleus to the cell periphery where the nucleus is defined as 0 and the distal cell membrane was 100) was graphed for cells with the FL construct (red line) and the ΔZIP construct (blue line). The FL mRNA extended to the cell periphery (red line). In contrast, the ΔZIP mRNA was concentrated in the area immediately around the nucleus and declined to the cell periphery (blue line). $n = 18$. (D) The sites of translation as a function of relative distance from the nucleus was graphed for a population of C2C12 cells containing the FL or ΔZIP constructs as in C. Consistent with the mRNA and protein localizations, the localization of translation sites for the FL construct showed translation of β-actin in the cell periphery, whereas the ΔZIP construct was confined to the perinuclear area. $n = 8$. (E) The total fluorescence intensity of the TC–GFP–β-actin was determined for a population of C2C12 cells containing the FL or ΔZIP construct as above. For the cells with FL construct, there was very little preference throughout the cytoplasm. In contrast, for cells with the ΔZIP construct, there was an enhanced signal closest to the nucleus with decreasing intensity peripherally. $n = 18$. Error bars are ± SEM.

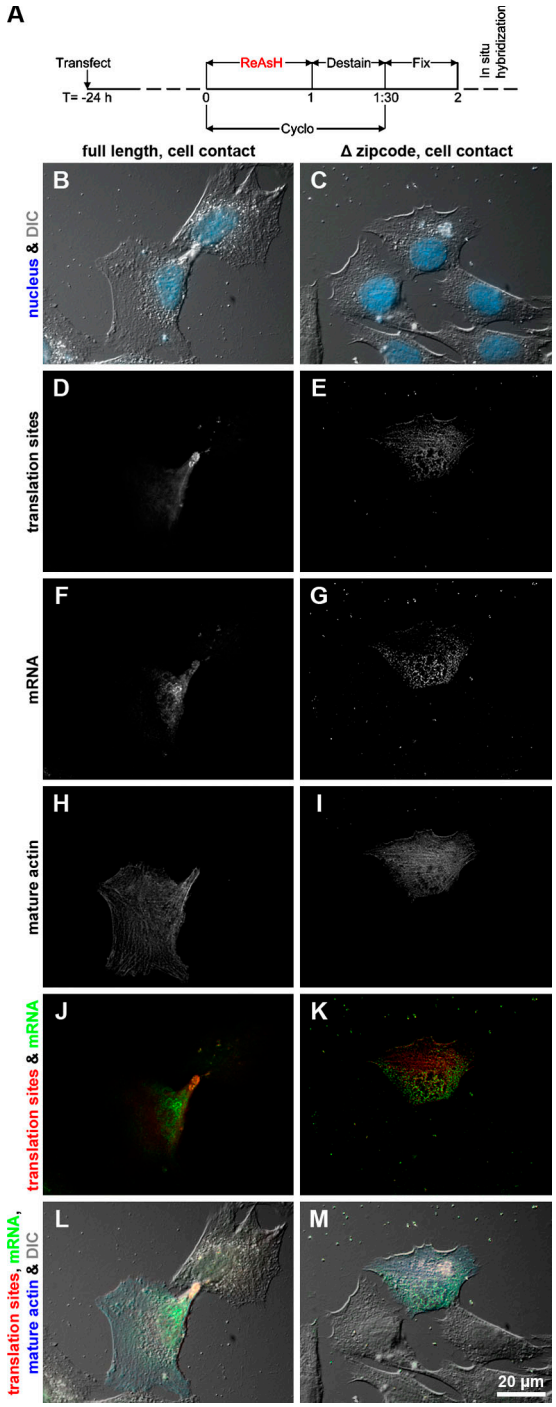

Figure 6. **Translation sites colocalize with their cognate mRNA near the sites of cell contact.** ReAsH staining experiments were performed on live cells that were subsequently fixed and processed for FISH, showing a colocalization between the red translation puncta and mRNA at cell contacts. Shown are contacting C2C12 cells containing either the FL construct (B, D, F, H, J, and L) or the ΔZIP construct (C, E, G, I, K, and M). The transfected cell exhibits positive GFP staining (H and I). (A) Schematic representation of the time course of the procedure. (B and C) DAPI staining and differential interference contrast (DIC) image overlaid. (D and E) A single plane of a deconvolved z series of C2C12 cells stained with ReAsH, showing sites of translation. Note that in the contacting cell (D) with the FL construct, the translation sites are restricted to the contact, whereas in E, translation sites are absent from the contact with the ΔZIP construct. (F and G) A single plane of a deconvolved z series of C2C12 cells hybridized with Cy-5–labeled probes against the GFP coding sequence, showing the distribution of the mRNA. (H and I) Deconvolved plane from a z series of C2C12 cells, showing GFP fluorescence from mature actin. (J and K) Overlay images of the translation site staining (red) and mRNA hybridizations (green). Note the colocalization of the translation sites and mRNA only at the contact with the FL construct (J) and the lack of colocalization with the ΔZIP construct (K). (L and M) Overlay of the translation site staining (red), mRNA hybridization (green), GFP actin fluorescence (blue), and differential interference contrast images.

were not observed at cell contacts (Fig. 6, right). Therefore, targeting of translation sites to cell contacts required the zipcode.

To investigate the fate of recently translated β-actin protein within the cell, pulse-chase staining of cells containing the FL or ΔZIP construct was performed, using FlAsH to bind up the unreacted TCs. After a short wash and a short pulse with ReAsH, the proteins synthesized during the ReAsH exposure could be evaluated (Gaietta et al., 2002). Images obtained in the red and green channels were presented as a ratio to determine where the β-actin synthesized during the chase period had accumulated (high red/green ratio). When cells in sparse culture, containing the FL construct, were examined, the majority of β-actin protein synthesized during the chase period was found at the perinuclear region and the leading edge of the cell (Fig. 7, B–D, red). When cells containing the FL construct were investigated by pulse-chase staining as they contacted other cells, the majority of the newly synthesized β-actin was localized at the perinuclear region and at the site of the cell contacts (Fig. 7, F–H, red), consistent with the observed translation at these sites (Fig. 6 J). Time-lapse images of cells illustrated that newly synthesized β-actin protein accumulated at cell contacts (Video 2, available at http://www.jcb.org/cgi/content/full/jcb.200512137/DC1). In contrast, newly synthesized β-actin from the ΔZIP transgene was primarily at the perinuclear region but failed to localize to cell contacts (Fig. 7, I–K), consistent with the lack of translation sites there (Fig. 6 K).

N-cadherin is lost from adherens junctions when β-actin translation is mislocalized

To assess the effect of mistargeting of β-actin translation on junction formation, we performed simultaneous ReAsH and N-cadherin staining on C2C12 cells. In contacting cells containing the FL transgene, which targets both translation sites and newly synthesized β-actin to the contact site, there was an enhancement of the amount of N-cadherin at the junction (Fig. 8, B and E). In contrast, contacting cells containing the ΔZIP transgene, which cannot target translation sites or newly synthesized β-actin, exhibit a decrease in the amount of N-cadherin at the junction (Fig. 8, A and E). When both populations were quantified and compared, there was an ∼33% decrease in the strength of the N-cadherin signal at the cell contacts when β-actin translation sites were mistargeted (Fig. 8 E).

Discussion

We report the novel use of labeled TC-tagged proteins to image specific nascent polypeptides during their synthesis in situ. We have used the TC system to detect polysomes in the process of synthesizing a specific polypeptide in real time with a spatial resolution of ∼0.2 μm. Our data demonstrate that peripheral

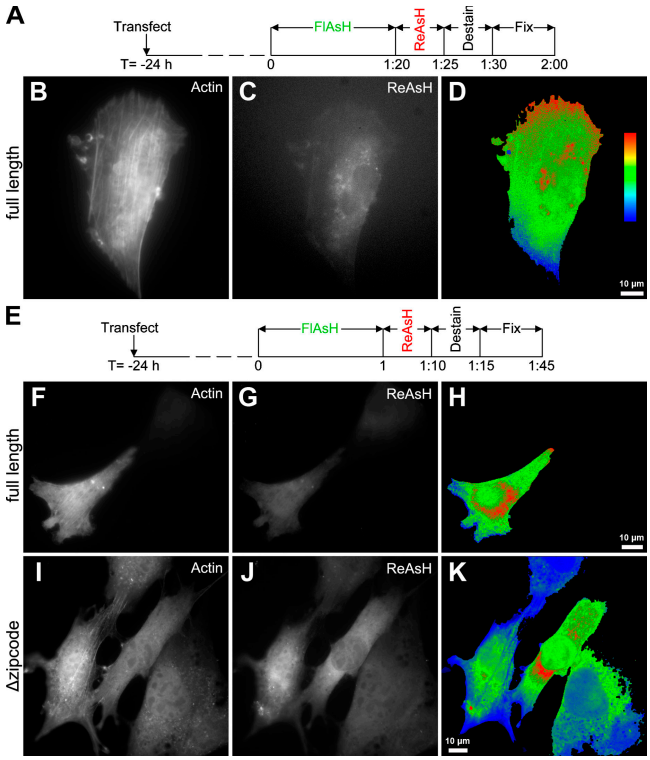

Figure 7. **Newly synthesized β-actin protein localizes to cell contacts and is zipcode dependent.** Cells were pulse labeled with FlAsH and chased with ReAsH to follow newly synthesized protein. (A) Schematic representation of the time course of the procedure used in B–D. (B–D) C2C12 cell containing the FL construct. (B) Epifluorescence image of a FlAsH-stained cell. (C) Epifluorescence image of a ReAsH-stained cell in B shown with the contrast stretched to enhance the low staining intensity. (D) Pseudocolored ratio image of C/B, where red indicates a higher red/green ratio. Notice that the β-actin synthesized during the chase period is localized to the perinuclear region and the leading edge of the cell. (E) Schematic representation of the time course of the procedure used in panels F–K. (F–G) C2C12 cell containing the FL construct touching an untransfected cell (not visible) at its tip. (F) Epifluorescence image of a FlAsH-stained cell. (G) Epifluorescence image of ReAsH-stained cell in F. (H) Pseudocolored ratio image of G/F. Note that the β-actin synthesized during the chase period is localized to the perinuclear region and the site of cell–cell contact. See Video 2 (available at http://www.jcb.org/cgi/content/full/jcb.200512137/DC1). (I–K) C2C12 cells containing the ΔZIP construct contacting other cells. (I) FlAsH-stained cells. (J) ReAsH-stained cells. (K) Pseudocolored ratio image of J/I. Notice that the majority of the β-actin synthesized during the chase period is localized to the perinuclear region with little protein accumulated at the sites of cell–cell contact. The highest ratios are shown in red, and the lowest ratios are shown in blue.

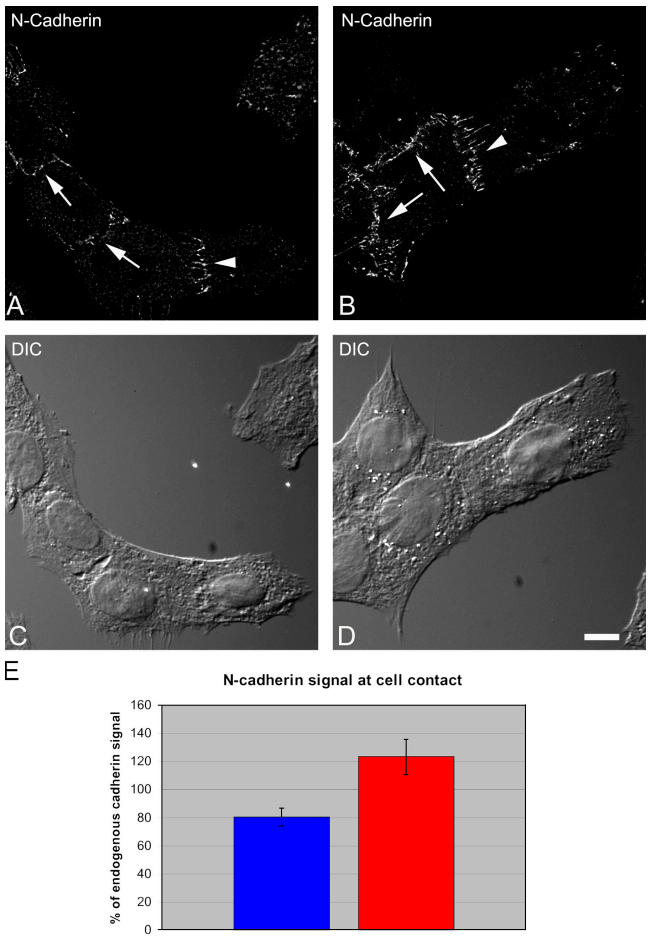

Figure 8. **N-cadherin is lost from adherens junction when the translation of β-actin is mislocalized.** (A) Indirect immunofluorescence image of N-cadherin staining of a cluster of C2C12 cells. The arrowheads point to the junction between a cell transfected with the ΔZIP or an FL construct. The arrows point to junctions between normal nontransfected cells. (B) N-cadherin staining of a cluster of C2C12 cells transfected with the FL transgene (arrowhead). (C) Differential interference contrast (DIC) image of the field shown in A. (D) Differential interference contrast image of the field shown in B. (E) Freehand regions of interest were drawn around the N-cadherin staining, and the mean fluorescence intensity of N-cadherin staining was determined using IPlab software. Quantification of the relative strength of N-cadherin staining was determined by comparing the ratio of the mean fluorescence intensity of N-cadherin at the junction with the mean fluorescence intensity of N-cadherin at the junctions between untransfected cells. The blue bar represents the ratio determined for cells containing the ΔZIP construct. The red bar represents the ratio determined for cells containing the FL construct. Eight fields of cells were compared for each construct. $P = 0.005$. Error bars are ± SEM.

translation of β-actin is zipcode dependent, as predicted by the localization of its mRNA (Hill and Gunning, 1993; Kislauskis et al., 1993). Mislocalization of β-actin mRNA using the ΔZIP construct resulted in the mislocalization of translation sites and, consequently, the newly synthesized protein. β-Actin translation sites were anchored and exhibit very little movement, providing a stable molecular framework for the observed accumulation of mature protein to specific subcellular compartments. In noncontacting cells, localized translation is seen at the leading lamella. In contrast, in contacting cells, localized translation is observed at sites of cell contact. When the trafficking of newly synthesized β-actin was monitored, accumulation of the protein at points of cell contact was only observed when the mRNA had a zipcode. This particular compartmentalization may have relevance because the actin cytoskeleton is actively involved in cell interactions, particularly in the fusion of myoblasts (Causeret et al., 2005).

The TC system has also been used to determine the temporal changes occurring at gap junctions using pulse-chase staining of newly synthesized connexins that were delivered to the plasma membrane containing junctional plaques composed of older connexin molecules (Gaietta et al., 2002). In addition, pulse-chase staining with FlAsH and ReAsH has been used to confirm that there is dendritic synthesis of GluR1 in response to extracellular stimuli using cultured neurons with physically

isolated dendrites (Ju et al., 2004). However, the translation site imaging technique allows the identification of the site where a specific mRNA is translated. We have been able to correlate the site of translation with the accumulation of the newly synthesized protein. This bridges the fields of mRNA localization and protein trafficking.

Evidence for local translation

The concept that translation can occur at distal sites within cells gained support with the discovery of polyribosomes localized to dendritic spines of hippocampal neurons (Steward and Levy, 1982). Subsequently, numerous studies using various reporter constructs and isolated dendritic cultures have demonstrated that local translation occurs within dendrites (Torre and Steward, 1992; Aakalu et al., 2001; Job and Eberwine, 2001; Macchi et al., 2003; Ju et al., 2004). Physically isolated dendrites were able to incorporate radio-labeled amino acids and were sensitive to puromycin (Torre and Steward, 1992). In addition, GFP reporters showed increased fluorescence in isolated dendritic cultures, supporting local translation (Aakalu et al., 2001; Job and Eberwine, 2001). However, there is an inherent drawback in GFP reporters. The fluorophore must undergo folding and oxidation, reported to take from 90 min to 4 h (Cubitt et al., 1995). Thus, there is a lag time between when these reporters are translated and when they can be detected. We have circumvented this issue by using reagents that fluoresce immediately upon their binding to the TC motif, which has allowed us a substantial improvement in spatial and temporal resolution in the intact cell.

Polysomes are directly visualized

After ReAsH staining, translation sites appear as bright puncta. Under normal conditions, it has been estimated that there is one ribosome per 90 nucleotides of coding sequence (Staehelin et al., 1964). For the β-actin construct, this would result in ∼21 ribosomes and nascent β-actin peptides per mRNA. When ribosomes are packed tightly in the presence of cycloheximide, they exhibit a maximum spacing of 1 ribosome per 30 nucleotides (Wolin and Walter, 1988), which would result in 63 ribosomes and nascent β-actin peptides per mRNA, providing a substantial TC signal at translation sites. The spatial amplification of fluorescence caused by staining the TC motifs at polysome sites allows for the detection of individual mRNAs in the process of translation. Analogously, using the spatial concentration of nascent RNA chains at their site of synthesis has been successfully used to detect single transcription sites based on hybridizing fluorescent oligonucleotide probes to nascent RNA transcripts in the nucleus (Femino et al., 1998) or the association of MS2-GFP to RNAs containing MS2 binding sites, allowing the detection of a single mRNA (Fusco et al., 2003; Shav-Tal et al., 2004).

Our fluorescent puncta have been characterized as translation sites based on several criteria. The size of the coding sequence for the transgene (1,884 bp) would produce a 565-nm mRNA if fully extended. The consistent size of the punctates suggests that the observed fluorescence is generated within a restricted volume. The sensitivity of these structures to puromycin indicates that intact polysomes are required for the detection of fluorescence signal. The enhancing effect of cycloheximide on the signal from the translation sites indicates that translational elongation must be inhibited to detect these sites for a prolonged period, to avoid runoff. The rate of signal loss (5 min) is consistent with estimates of the rate of translation (∼1 amino acid per second per ribosome or ∼10 min for our construct), calculated using several in vitro methods (Lodish and Jacobson, 1972; Palmiter, 1972; Vanzi et al., 2003).

Translation sites of β-actin are localized by the zipcode

The localization of translation sites is consistent with the recent observation that zipcode binding protein 1 (ZBP1) has an additional role as a translational inhibitor (Huttelmaier et al., 2005). ZBP1 was originally characterized as a transacting factor capable of binding the zipcode sequence that was required for the proper localization of β-actin mRNA to the leading edge of fibroblasts and to the growth cones of neurites (Kislauskis et al., 1993; Zhang et al., 1999; Huttelmaier et al., 2005). The ZBP1–β-actin mRNA complex, formed in the nucleus before mRNA export, is incapable of translation until ZBP1 is phosphorylated by Src at the cell periphery, resulting in the dissociation of the mRNA from ZBP1 (Huttelmaier et al., 2005). Thus, the localization of translation sites at the perinuclear region for cells containing the β-actin construct without the zipcode is consistent with the hypothesis that ZBP1 is required to inhibit translation until the mRNA has reached its final destination at the cell periphery.

Locally translated β-actin accumulates into specialized structures and may generate storage compartments

It has been observed that injection of fluorescently labeled actin into cells results in a rapid diffusion of fluorescence throughout the cell (Wang et al., 1982). Therefore, the production of β-actin from localized mRNA may be critical for concentration of the protein at sites of β-actin polymerization (Shestakova et al., 2001). We observed the local translation and accumulation of β-actin at cell contacts. The majority of β-actin mRNAs are not actively translating outside of the regions of cell contact, indicating that the distribution of a particular mRNA alone may not be indicative of where protein synthesis and product accumulation occurs. Consistent with this, RhoA is up-regulated at cell–cell contacts and is responsible for the localization of β-actin mRNA in fibroblasts (Latham et al., 2001; Charrasse et al., 2002). It has been shown that β-actin mRNA is often localized to cell contacts at the base of processes that are morphologically similar to filopodia at nascent adherens junctions (Lawrence and Singer, 1986; Yonemura et al., 1995; Vasioukhin et al., 2000). At cadherin-mediated cell contacts, the up-regulation of RhoA leads to the recruitment of β-catenin, β-actin mRNA, and newly synthesized protein after the local translation of the mRNA. Presumably, this provides the molecular building blocks for adherens junction formation at a discrete cytoplasmic site (Charrasse et al., 2002). Actin polymerization is required for adherens junction formation, as these structures

fail to form in the presence of cytochalasin D (Vasioukhin et al., 2000). At putative adherens junctions, the multiprotein complex of cadherin and β-catenin is found in close proximity to barbed ends of actin, the distribution of which is in turn dependent on the localization of β-actin mRNA (Adams et al., 1998; Shestakova et al., 2001). Thus, the mislocalization of β-actin mRNA through the deletion of the zipcode sequence results in the mislocalization of newly synthesized protein (Fig. 7) and may result in a failure of barbed ends to form at cell contacts, ultimately affecting contact stability.

Recent work identified two spatially distinct populations of actin filaments at cell–cell contacts called junctional actin and peripheral thin bundles (Zhang et al., 2005). Junctional actin was characterized as dynamic, with polymerization occurring at barbed ends from a postulated stored G-actin pool that was not affected by Ca^{2+} levels, resulting in the stabilization of clustered cadherin receptors (Zhang et al., 2005). The intensity of N-cadherin staining at cell contacts was reduced by ∼33% in the cells with mislocalized β-actin mRNA and translation sites (Fig. 8). Thus, the mislocalization of newly translated β-actin and barbed ends resulted in a decrease in junctional actin and, ultimately, decreased cadherin staining at the adherens junction. These data provide evidence for the importance of compartmentalized synthesis of β-actin on the formation and/or maintenance of peripherally localized multiprotein complexes such as adherens junctions (Fig. 8). Reduced expression and mislocalization of cadherin have also been observed in *Drosophila melanogaster* Myosin VI–deletion mutants, resulting in aberrant border cell migration and dorsal closure (Geisbrecht and Montell, 2002; Millo et al., 2004). Our data suggest that mistargeting of β-actin through mislocalization of its translation sites effectively knocks down the protein at its functional site and affects the distribution of other proteins at these sites.

β-Actin that is translated locally may have some inherent mechanism for remaining in the region where it is synthesized. Possibly, recently synthesized β-actin incorporates into nearby actin filaments and forms macromolecular complexes with other actin binding proteins in the region of the translation sites. Actin at the leading edge of motile cells interacts with different actin binding proteins and exhibits different rates of assembly and disassembly and different treadmilling rates, suggesting a spatial control of actin dynamics (Shuster and Herman, 1995; DesMarais et al., 2002; Gupton et al., 2005). Moreover, the local synthesis of β-actin may populate a novel compartment of nonfilamentous actin at the cell periphery identified by vitamin D binding protein staining (Cao et al., 1993). This could allow for rapid actin polymerization at the cellular periphery in response to extracellular cues. Several proteins thought to function at the cell periphery seem to have a preference for β-actin, including ezrin (Shuster and Herman, 1995), profilin (Segura and Lindberg, 1984), thymosin β 4 (Weber et al., 1992), and L-plastin (Namba et al., 1992). Many of these proteins associated with actin contain zipcodes within the 3′UTRs of their mRNAs, suggesting a coordinated translation- and localization-regulated pathway (Mingle et al., 2005). Thus, information contained within untranslated regions of mRNAs coordinates mRNA localization, local translation, and ultimately the distribution of newly synthesized proteins. The approach described here allows a rigorous testing of the hypothesis that localized synthesis of proteins affects cell structure and function.

Materials and methods

Materials

FlAsH and ReAsH were a gift from R. Tsien (University of California, San Diego, La Jolla, CA) and were later purchased from Invitrogen under the trade names lumio green and lumio red, respectively.

β-Actin plasmid constructs

A PCR primer was synthesized containing a HindIII restriction site, the coding sequence for a TC tag, and sequences complementary to the GFP coding region called TC1, 5′-tggaagcttccaccatgtgggattgttgtccaggatgttgtaaaatggtgagcaagggcgaggagctgttc-3′. An additional primer called TC2, 5′-tggaagcttccaccatgttcctcaactgctgcccaggatgttgtatggagccatggtgagcaagggcgaggagctgttc-3′, was synthesized. A third PCR primer was synthesized containing a BamHI restriction site and sequence complementary to the GFP coding region 5′-ccggatcccttgtacagctcgtccatgc-3′. The primers were used to amplify the GFP coding sequence from plasmid pβ-actin EGFP (Ballestrem et al., 1998) with a TC motif MWDCCPGCCKM (from the TC1 primer; Figs. 2–5 and 7) or the improved TC motif MFLNCCPGCCMEP (from the TC2 primer; Figs. 1 and 6) at the N terminus (Martin et al., 2005). The EGFP coding sequence was removed from plasmid pβ-actin EGFP using the restriction enzymes BamHI and HindIII and replaced with the TC-containing EGFP PCR product to produce the plasmid TC–GFP–β-actin with no zipcode (ΔZIP). To produce the FL β-actin plasmid, the ΔZIP plasmid was cut with BamHI and XbaI to remove the β-actin coding sequence. A second plasmid containing the β-actin coding sequence with a zipcode was also cut with BamHI and XbaI, and this product was ligated into the cut ΔZIP plasmid to produce the TC–GFP–β-actin FL plasmid.

Cell culture

C2C12 mouse myoblast cells were cultured in α-MEM media with 10% FBS using standard techniques. For imaging experiments, C2C12 cells were plated directly onto 35- × 10-mm plastic tissue culture dishes or onto acid-washed glass coverslips 24 h before transfection. The TC–GFP–β-actin constructs were transfected into the C2C12 cells using Fugene 6 transfection reagent (Roche Diagnostics Corporation) according to the manufacturer's instructions for 24 h at 37°C. After the incubation, the Fugene 6 solution was removed and replaced with α-MEM media supplemented with 10% FBS for 1 h at 37°C before cells were used in experiments.

FlAsH and ReAsH staining and detection

Transfected C2C12 cells were treated with 100 μg/ml cycloheximide ready-made solution (Sigma-Aldrich) for 30 min at 37°C. The cells were then treated with 1× staining solution (1 μM FlAsH or 2.5 μM ReAsH in 1 ml of Opti-MEM medium (Invitrogen), 100 μg/ml cycloheximide solution, and 10 μM ethanedithiol (EDT_2) for 15 min to 2 h at room temperature. The cells were washed in Opti-MEM followed by destaining in 250 μM EDT_2, 100 μg/ml cycloheximide, and 1 ml of Opti-MEM for 5–30 min at room temperature. The cells were washed in Opti-MEM, and digital images were acquired using an epifluorescence microscope (BX61; Olympus) with a UPlanApo 60×/1.2 NA W PSF (water immersion; Olympus) objective for live cell imaging or a PlanApo 60×/1.4 NA oil-immersion objective (Olympus) for fixed cells and a 100-Watt mercury arc lamp (Olympus), equipped with a camera (CoolSNAP HQ; Photometrics) using IPLab software (Windows v3; BD Biosciences) and filter sets 41001 (FITC), 41007 (Cy3), 41004 (ReAsH), 41008 (Cy5), and SP104v1 (Cy5 narrow band pass; Chroma Technology Corp.).

Translational inhibitor studies

C2C12 cells containing the FL construct were treated with 200 μg/ml puromycin for 30 min followed by 30 min of ReAsH staining in the presence of 100 μg/ml cycloheximide. As a control, C2C12 cells containing the FL construct that were not treated with puromycin were stained for 30 min in ReAsH in the presence of 100 μg/ml cycloheximide. The number of translation sites per cell was determined for the untreated and puromycin-treated populations of C2C12 cells.

ReAsH washout experiments

C2C12 cells containing the FL plasmid were stained with ReAsH in the absence of cycloheximide. After destaining, the cells were imaged using a Cy3 filter set at 1 image/min. As a control, C2C12 cells containing the FL plasmid were stained with ReAsH in the presence of cycloheximide, washed, and imaged using a Cy3 filter set.

FISH staining and intensity distribution analysis

C2C12 cells containing either the FL or the ΔZIP plasmids were hybridized with a Cy5-labeled antisense probe to the GFP coding sequence (Femino et al., 2003). The antisense GFP probe is a mixture of three oligonucleotides with the following sequences: GFP-1, GGGTCTTGTAGTTGCCGTCGTCCTTGAAGAAGATGGTGCG; GFP-2, GGCTGTTGTAGTTGTACTCCAGCTTGTGCCCCAGGATGTT; and GFP-3, TCTTTGCTCAGGGCGGACTGGGTGCTCAGGTAGTGGTTGT. Images were obtained using a Cy5 filter set. The intracellular distribution of FISH signal was determined using software written to measure the total fluorescence intensity as a function of distance from the nucleus. The software identified the nuclear boundary using an overlaid and registered image of the DAPI-counterstained nucleus. The software identified the cellular boundary using an edge-detection routine with user-adjustable parameters. The cytoplasmic area was defined as the region between the nuclear and cellular boundaries identified. The FISH signal in the entire cytoplasmic area was analyzed by the software, which outputted a histogram of FISH intensity as a function of distance from the nucleus. The data were normalized by total FISH intensity and longest distance from the nuclear to cellular boundary.

ReAsH and FISH staining

C2C12 cells containing the FL or ΔZIP constructs were stained with ReAsH, fixed in 4% paraformaldehyde for 30 min at room temperature, and processed for FISH using a Cy5-labeled probe to the GFP coding sequence (Femino et al., 1998). Images were obtained using the FITC, ReAsH, and Cy5 narrow filter sets and deconvolved using Huygens Professional version 2.6.4 (Scientific Volume Imaging). Colocalization between the ReAsH and FISH images was determined by overlaying individual planes from each channel using IPlab software.

Pulse-chase staining and ratio imaging

50% confluent C2C12 cells containing the FL or ΔZIP constructs were pulsed with 1 μM FlAsH in 1 ml of Opti-MEM and 10 μM EDT_2 for 1 h at 37°C. The cells were then chased with 2.5 μM ReAsH in 1 ml of Opti-MEM and 10 μM EDT_2 for 15 min at 37°C. A 5-min destain in 250 μM EDT_2 in 1 ml of Opti-MEM was performed, and cells were imaged for live cell experiments or fixed in 4% paraformaldehyde in 1% PBS. For each cell, an image was obtained using the FITC and ReAsH filter sets. Ratio image analysis was performed using software that generated a binary mask of the denominator image by taking all pixel values greater than a fixed value. To this binary mask, we apply a grayscale closing operation (dilation followed by erosion) using a 4×4 matrix where each element is 1. The resulting mask defines the region of the cell that has an adequate signal/noise ratio. The ratio of the original background-subtracted images is then calculated in regions defined by the binary mask. The ReAsH image is the numerator, and the FlAsH image is the denominator.

ReAsH and immunofluorescence staining

ReAsH staining was performed followed by fixation in 4% paraformaldehyde in 1% PBS. The samples were blocked in 3% BSA, stained in a 1:50 dilution of anti–N-cadherin antibodies for 3 h at room temperature (BD Biosciences), and stained in a 1:250 dilution of Cy5-labeled anti-mouse secondary antibody. Images were obtained using the FITC, ReAsH, and Cy5 narrow filter sets.

Online supplemental material

Fig. S1 demonstrates that translation sites are resistant to detergent extraction, suggesting an interaction with the cytoskeleton. Video 1 shows a C2C12 cell that was stained with ReAsH; an image was collected every 5 min for 1 h at room temperature. Video 2 shows a C2C12 cell transfected with the FL construct contacting an adjacent cell pulse labeled with FlAsH for 1 h and chase labeled with ReAsH for 15 min. Online supplemental material is available at http://www.jcb.org/cgi/content/full/jcb.200512137/DC1.

We thank Dan Larson for programming the ratio imaging software and stimulating discussion. We also thank Amber Wells for helpful comments and for measuring the rates of mRNA movements in C2C12 cells. In addition, we would like to thank Roger Tsien for the generous gift of ReAsH.

The research was supported by National Institutes of Health grant AR41480 to R.H. Singer and National Institutes of Health minority postdoctoral research supplements AR41480 to A.J. Rodriguez and CA100324 to J. Condeelis.

Submitted: 27 December 2005
Accepted: 5 September 2006

References

Aakalu, G., W.B. Smith, N. Nguyen, C. Jiang, and E.M. Schuman. 2001. Dynamic visualization of local protein synthesis in hippocampal neurons. *Neuron.* 30:489–502.

Adams, C.L., Y.T. Chen, S.J. Smith, and W.J. Nelson. 1998. Mechanisms of epithelial cell-cell adhesion and cell compaction revealed by high-resolution tracking of E-cadherin-green fluorescent protein. *J. Cell Biol.* 142:1105–1119.

Ballestrem, C., B. Wehrle-Haller, and B.A. Imhof. 1998. Actin dynamics in living mammalian cells. *J. Cell Sci.* 111:1649–1658.

Bashirullah, A., R.L. Cooperstock, and H.D. Lipshitz. 1998. RNA localization in development. *Annu. Rev. Biochem.* 67:335–394.

Cao, L.G., D.J. Fishkind, and Y.L. Wang. 1993. Localization and dynamics of nonfilamentous actin in cultured cells. *J. Cell Biol.* 123:173–181.

Causeret, M., N. Taulet, F. Comunale, C. Favard, and C. Gauthier-Rouviere. 2005. N-cadherin association with lipid rafts regulates its dynamic assembly at cell-cell junctions in C2C12 myoblasts. *Mol. Biol. Cell.* 16:2168–2180.

Charrasse, S., M. Meriane, F. Comunale, A. Blangy, and C. Gauthier-Rouviere. 2002. N-cadherin-dependent cell-cell contact regulates Rho GTPases and β-catenin localization in mouse C2C12 myoblasts. *J. Cell Biol.* 158:953–965.

Cubitt, A.B., R. Heim, S.R. Adams, A.E. Boyd, L.A. Gross, and R.Y. Tsien. 1995. Understanding, improving and using green fluorescent proteins. *Trends Biochem. Sci.* 20:448–455.

DesMarais, V., I. Ichetovkin, J. Condeelis, and S.E. Hitchcock-DeGregori. 2002. Spatial regulation of actin dynamics: a tropomyosin-free, actin-rich compartment at the leading edge. *J. Cell Sci.* 115:4649–4660.

Femino, A.M., F.S. Fay, K. Fogarty, and R.H. Singer. 1998. Visualization of single RNA transcripts in situ. *Science.* 280:585–590.

Femino, A.M., K. Fogarty, L.M. Lifshitz, W. Carrington, and R.H. Singer. 2003. Visualization of single molecules of mRNA in situ. *Methods Enzymol.* 361:245–304.

Fusco, D., N. Accornero, B. Lavoie, S.M. Shenoy, J.M. Blanchard, R.H. Singer, and E. Bertrand. 2003. Single mRNA molecules demonstrate probabilistic movement in living mammalian cells. *Curr. Biol.* 13:161–167.

Gaietta, G., T.J. Deerinck, S.R. Adams, J. Bouwer, O. Tour, D.W. Laird, G.E. Sosinsky, R.Y. Tsien, and M.H. Ellisman. 2002. Multicolor and electron microscopic imaging of connexin trafficking. *Science.* 296:503–507.

Geisbrecht, E.R., and D.J. Montell. 2002. Myosin VI is required for E-cadherin-mediated border cell migration. *Nat. Cell Biol.* 4:616–620.

Godchaux, W., III, S.D. Adamson, and E. Herbert. 1967. Effects of cycloheximide on polyribosome function in reticulocytes. *J. Mol. Biol.* 27:57–72.

Gupton, S.L., K.L. Anderson, T.P. Kole, R.S. Fischer, A. Ponti, S.E. Hitchcock-DeGregori, G. Danuser, V.M. Fowler, D. Wirtz, D. Hanein, and C.M. Waterman-Storer. 2005. Cell migration without a lamellipodium: translation of actin dynamics into cell movement mediated by tropomyosin. *J. Cell Biol.* 168:619–631.

Hill, M.A., and P. Gunning. 1993. β and γ actin mRNAs are differentially located within myoblasts. *J. Cell Biol.* 122:825–832.

Hofer, D., W. Ness, and D. Drenckhahn. 1997. Sorting of actin isoforms in chicken auditory hair cells. *J. Cell Sci.* 110:765–770.

Huttelmaier, S., D. Zenklusen, M. Lederer, J. Dictenberg, M. Lorenz, X. Meng, G.J. Bassell, J. Condeelis, and R.H. Singer. 2005. Spatial regulation of beta-actin translation by Src-dependent phosphorylation of ZBP1. *Nature.* 438:512–515.

Job, C., and J. Eberwine. 2001. Localization and translation of mRNA in dendrites and axons. *Nat. Rev. Neurosci.* 2:889–898.

Joklik, W.K., and Y. Becker. 1965. Studies on the genesis of polyribosomes. I. Origin and significance of the subribosomal particles. *J. Mol. Biol.* 13:496–510.

Ju, W., W. Morishita, J. Tsui, G. Gaietta, T.J. Deerinck, S.R. Adams, C.C. Garner, R.Y. Tsien, M.H. Ellisman, and R.C. Malenka. 2004. Activity-dependent regulation of dendritic synthesis and trafficking of AMPA receptors. *Nat. Neurosci.* 7:244–253.

Kislauskis, E.H., Z. Li, R.H. Singer, and K.L. Taneja. 1993. Isoform-specific 3′-untranslated sequences sort α-cardiac and β-cytoplasmic actin messenger RNAs to different cytoplasmic compartments. *J. Cell Biol.* 123:165–172.

Kislauskis, E.H., X. Zhu, and R.H. Singer. 1994. Sequences responsible for intracellular localization of β-actin messenger RNA also affect cell phenotype. *J. Cell Biol.* 127:441–451.

Kislauskis, E.H., X. Zhu, and R.H. Singer. 1997. β-Actin messenger RNA localization and protein synthesis augment cell motility. *J. Cell Biol.* 136:1263–1270.

Latham, V.M., E.H. Yu, A.N. Tullio, R.S. Adelstein, and R.H. Singer. 2001. A Rho-dependent signaling pathway operating through myosin localizes beta-actin mRNA in fibroblasts. *Curr. Biol.* 11:1010–1016.

Lawrence, J.B., and R.H. Singer. 1986. Intracellular localization of messenger RNAs for cytoskeletal proteins. *Cell.* 45:407–415.

Lenk, R., L. Ransom, Y. Kaufmann, and S. Penman. 1977. A cytoskeletal structure with associated polyribosomes obtained from HeLa cells. *Cell.* 10:67–78.

Lodish, H.F. 1971. Alpha and beta globin messenger ribonucleic acid. Different amounts and rates of initiation of translation. *J. Biol. Chem.* 246:7131–7138.

Lodish, H.F., and A. Jacobson. 1972. Translational control of protein synthesis in eukaryotic cells: is there tissue or species specificity of the translational apparatus? *Dev. Biol.* 27:283–285.

Macchi, P., I. Hemraj, B. Goetze, B. Grunewald, M. Mallardo, and M.A. Kiebler. 2003. A GFP-based system to uncouple mRNA transport from translation in a single living neuron. *Mol. Biol. Cell.* 14:1570–1582.

Martin, B.R., B.N.G. Giepmans, S.R. Adams, and R.Y. Tsien. 2005. Mammalian cell-based optimization of the biarsenical-binding tetracysteine motif for improved fluorescence and affinity. *Nat. Biotechnol.* 23:1308–1314.

Millo, H., K. Leaper, V. Lazou, and M. Bownes. 2004. Myosin VI plays a role in cell-cell adhesion during epithelial morphogenesis. *Mech. Dev.* 121:1335–1351.

Mingle, L.A., N.N. Okuhama, J. Shi, R.H. Singer, J. Condeelis, and G. Liu. 2005. Localization of all seven messenger RNAs for the actin-polymerization nucleator Arp2/3 complex in the protrusions of fibroblasts. *J. Cell Sci.* 118:2425–2433.

Namba, Y., M. Ito, Y. Zu, K. Shigesada, and K. Maruyama. 1992. Human T cell L-plastin bundles actin filaments in a calcium-dependent manner. *J. Biochem. (Tokyo).* 112:503–507.

Palmiter, R.D. 1972. Regulation of protein synthesis in chick oviduct. II. Modulation of polypeptide elongation and initiation rates by estrogen and progesterone. *J. Biol. Chem.* 247:6770–6780.

Rodriguez, A.J., S.A. Seipel, D.R. Hamill, D.P. Romancino, M. Di Carlo, K.A. Suprenant, and E.M. Bonder. 2005. Seawi–a sea urchin piwi/argonaute family member is a component of MT-RNP complexes. *RNA.* 11:646–656.

Segura, M., and U. Lindberg. 1984. Separation of non-muscle isoactins in the free form or as profilactin complexes. *J. Biol. Chem.* 259:3949–3954.

Shav-Tal, Y., R.H. Singer, and X. Darzacq. 2004. Imaging gene expression in single living cells. *Nat. Rev. Mol. Cell Biol.* 5:855–861.

Shestakova, E.A., J. Wyckoff, J. Jones, R.H. Singer, and J. Condeelis. 1999. Correlation of beta-actin messenger RNA localization with metastatic potential in rat adenocarcinoma cell lines. *Cancer Res.* 59:1202–1205.

Shestakova, E.A., R.H. Singer, and J. Condeelis. 2001. The physiological significance of beta-actin mRNA localization in determining cell polarity and directional motility. *Proc. Natl. Acad. Sci. USA.* 98:7045–7050.

Shuster, C.B., and I.M. Herman. 1995. Indirect association of ezrin with F-actin: isoform specificity and calcium sensitivity. *J. Cell Biol.* 128:837–848.

Singer, R.H., and S. Penman. 1972. Stability of HeLa cell mRNA in actinomycin. *Nature.* 240:100–102.

Staehelin, T., F.O. Wettstein, H. Oura, and H. Noll. 1964. Determination of the coding ratio based on molecular weight of messenger ribonucleic acid associated with ergosomes of different aggregate size. *Nature.* 201:264–270.

Steward, O., and W.B. Levy. 1982. Preferential localization of polyribosomes under the base of dendritic spines in granule cells of the dentate gyrus. *J. Neurosci.* 2:284–291.

Sundell, C.L., and R.H. Singer. 1990. Actin mRNA localizes in the absence of protein synthesis. *J. Cell Biol.* 111:2397–2403.

Tiruchinapalli, D.M., Y. Oleynikov, S. Kelic, S.M. Shenoy, A. Hartley, P.K. Stanton, R.H. Singer, and G.J. Bassell. 2003. Activity-dependent trafficking and dynamic localization of zipcode binding protein 1 and beta-actin mRNA in dendrites and spines of hippocampal neurons. *J. Neurosci.* 23:3251–3261.

Torre, E.R., and O. Steward. 1992. Demonstration of local protein synthesis within dendrites using a new cell culture system that permits the isolation of living axons and dendrites from their cell bodies. *J. Neurosci.* 12:762–772.

Vanzi, F., S. Vladimirov, C.R. Knudsen, Y.E. Goldman, and B.S. Cooperman. 2003. Protein synthesis by single ribosomes. *RNA.* 9:1174–1179.

Vasioukhin, V., C. Bauer, M. Yin, and E. Fuchs. 2000. Directed actin polymerization is the driving force for epithelial cell-cell adhesion. *Cell.* 100:209–219.

Wang, W., S. Goswami, K. Lapidus, A.L. Wells, J.B. Wyckoff, E. Sahai, R.H. Singer, J.E. Segall, and J.S. Condeelis. 2004. Identification and testing of a gene expression signature of invasive carcinoma cells within primary mammary tumors. *Cancer Res.* 64:8585–8594.

Wang, Y.L., F. Lanni, P.L. McNeil, B.R. Ware, and D.L. Taylor. 1982. Mobility of cytoplasmic and membrane-associated actin in living cells. *Proc. Natl. Acad. Sci. USA.* 79:4660–4664.

Weber, A., V.T. Nachmias, C.R. Pennise, M. Pring, and D. Safer. 1992. Interaction of thymosin beta 4 with muscle and platelet actin: implications for actin sequestration in resting platelets. *Biochemistry.* 31:6179–6185.

Wolin, S.L., and P. Walter. 1988. Ribosome pausing and stacking during translation of a eukaryotic mRNA. *EMBO J.* 7:3559–3569.

Yarmolinsky, M.B., and G.L. De la Haba. 1959. Inhibition of puromycin of amino acid incorporation into protein. *Proc. Natl. Acad. Sci. USA.* 45:1721–1727.

Yonemura, S., M. Itoh, A. Nagafuchi, and S. Tsukita. 1995. Cell-to-cell adherens junction formation and actin filament organization: similarities and differences between non-polarized fibroblasts and polarized epithelial cells. *J. Cell Sci.* 108:127–142.

Zhang, H.L., R.H. Singer, and G.J. Bassell. 1999. Neurotrophin regulation of β-actin mRNA and protein localization within growth cones. *J. Cell Biol.* 147:59–70.

Zhang, H.L., T. Eom, Y. Oleynikov, S.M. Shenoy, D.A. Liebelt, J.B. Dictenberg, R.H. Singer, and G.J. Bassell. 2001. Neurotrophin-induced transport of a beta-actin mRNP complex increases beta-actin levels and stimulates growth cone motility. *Neuron.* 31:261–275.

Zhang, J., R.E. Campbell, A.Y. Ting, and R.Y. Tsien. 2002. Creating new fluorescent probes for cell biology. *Nat. Rev. Mol. Cell Biol.* 3:906–918.

Zhang, J., M. Betson, J. Erasmus, K. Zeikos, M. Bailly, L.P. Cramer, and V.M. Braga. 2005. Actin at cell-cell junctions is composed of two dynamic and functional populations. *J. Cell Sci.* 118:5549–5562.